Microsyst Technol (2012) 18:481–488
DOI 10.1007/s00542-012-1425-0

TECHNICAL PAPER

Rubber-assisted embossing of polymer thin films using molds with through-thickness microchannels

Danyang Zhao · Tom Wyatt · Minjie Wang · Allen Yi · Donggang Yao

Received: 2 December 2011 / Accepted: 6 January 2012 / Published online: 24 January 2012

Abstract A flexible microfluidic chip is difficult to fabricate using the standard hot embossing technology. In this study, rubber-assisted embossing of polymer thin films using molds with through-thickness microchannels was investigated. The polymer film was thermoformed into the microchannels by rubber as a soft counter-tool. Different processing conditions, as well as material selections, affecting the thickness uniformity and replicated depth were examined. Results indicated that smoother surfaces on the embossed articles were created, and the thickness uniformity and the depth of the embossed channel were significantly affected by the embossing temperature, the embossing pressure, and the rubber hardness. The embossed film was sealed on one side with a layer of transparent adhesive film to form closed microchannels, and desired 3-D flow characteristics were obtained with this flexible microfluidic chip.

1 Introduction

A strongly increasing demand for micro, total analysis systems such as capillary electrophoresis systems requires the development of low priced, i.e., simple and fast, methods for manufacturing hollow microfluidic structures from polymers, preferably for single use. Existing approaches are based on fabricating plastic microstructures by injection molding or hot embossing and subsequent covering of the molded structures with plastic films or sheets (Schift et al. 2000; Narasimhan and Papautsky 2004; Gates et al. 2005; Rowland et al. 2005). However, the current micro molding techniques are mostly designed for surface microstructures and therefore are ineffective or even incapable in fabricating microchannels on a thin plastic film (Nagarajan and Yao 2009). Micrometer thick shell structures are difficult to fill by injection molding because of the extremely thin wall section and the extremely high length-to-thickness ratio. Furthermore, exceedingly high residual stresses may be developed during such ultra-thin wall molding, deteriorating the part quality. Comparing to injection molding, hot embossing is especially useful for feature transfer from microstructured flat and hard surfaces to thermoplastic polymer films (Dreuth and Heiden 1999; Truckenmuller et al. 2002; Taylor et al. 2010). However, in its standard setup, hot embossing is not suitable for handling shell-type micropatterns either. If a matching pair of hard tools is used for defining the shell geometry, the process is subjected to misalignment issues and processing difficulties.

Recently, a rubber-assisted hot embossing process for shell patterning was investigated (Nagarajan and Yao 2011a, b). Compared with the standard hot embossing process, this method eliminates the practical difficulty in applying a matching pair of hard mold surfaces to define the geometry of the shell pattern throughout the thickness. The rubber pad essentially works as a deformable and recoverable soft counter-tool. This can help protect the embossing master, build up more uniform embossing pressure, and achieve ease of demolding.

D. Zhao (✉) · M. Wang
Dalian University of Technology, Dalian,
People's Republic of China
e-mail: zhaody@dlut.edu.cn

D. Zhao · T. Wyatt · D. Yao (✉)
Georgia Institute of Technology,
Atlanta, GA, USA
e-mail: yao@gatech.edu

A. Yi
The Ohio State University, Columbus,
OH, USA

In this study, the rubber-assisted hot embossing process was further developed to better utilize the thermoforming characteristics of this process. Instead of microcavities with depths, through-thickness microchannels were machined on the mold by micro wire electrical discharge machine (EDM) open to the atmosphere on the back side of the mold. The resulting process is particularly useful for fabrication microchannel patterns. During embossing, the embossing film is forced by the rubber into the open microchannels on the mold, reassembling a positive pressure thermoforming process. This modification not only simplifies the mold design and fabrication, but also creates smoother surfaces on the embossed articles. Furthermore, air in the mold cavity can freely escape during embossing, thus eliminating any adverse effect caused by compressed air in the mold cavity. Different processing conditions and material selections, affecting the thickness uniformity and replicated depth, were investigated. The channel uniformity was examined by covering the microchannel with a layer of transparent film and injecting colored water.

2 Experimental

2.1 Materials

Biaxially stretched polystyrene (PS) film with a thickness of 25 μm obtained from Goodfellow Corporation was used as an embossing film. The glass transition temperature (Tg) given by the material supplier is 100°C. Different grades of high-temperature silicone rubber sheets with a thickness of 6.4 mm were obtained from McMaster-Carr Supply Company. The Shore hardness of these rubber sheets varies from 20 to 60 A. They were cut into circular pads of diameter 56 mm and directly used as soft counter-tools.

2.2 Embossing setup

As shown in Fig. 1, rubber-assisted hot embossing follows a similar sequence of operation as standard hot embossing, i.e., mold preheating, embossing, holding, cooling, and demolding. Two hydraulic presses from CARVER Corporation equipped with heated lower and upper platens were used as a hot embossing apparatus. One press is for preheating, and the other is for embossing and cooling. The two-step method eliminates the lengthy thermal cycling of a single mold. Deformation of the PS film and the rubber pad during the embossing and holding stages was performed under constant pressure control with varied embossing pressure between 0.5 and 3.0 MPa. The embossing temperature was also varied in the experiments, from 90 to 120°C. These bounds for the process window were determined by initial sensitivity tests of the process.

A stainless-steel stamp (56 mm in diameter and 10 mm in thickness) with a U-shaped through-thickness microchannel was used as an embossing mold. To fabricate this stamp, the steel was first precision ground and then machined using a micro wire EDM process, with a wire diameter of 50 μm. The geometry and dimension of the microchannel is shown in Fig. 2a. The microchannel is approximately 280 μm wide and through the thickness. The diameters of the two end holes are approximately 3.0 mm. A photo of the actual stamp is given in Fig. 2b.

2.3 Characterization

The thermomechanical properties of the PS film and the different grades of rubber pads were characterized using dynamical mechanical analysis (DMA) (TA Instruments, Model No. Q800). The DMA tests were performed in a small-strain temperature-sweeping mode for characterizing the linear viscoelastic properties. The testing frequency and strain amplitude were fixed at 1 Hz and 1%, respectively. Furthermore, the PS film was characterized using hot-chamber tensile testing (INSTRON, Model No. 5566). The thickness uniformity and channel depth of the embossed PS film were examined using stereo optical microscopy (OLYMPUS, Model No. BX51SMZ). The surface roughness was examined using scanning electron microscopy (SEM) (HITACHI, Model No. S-800).

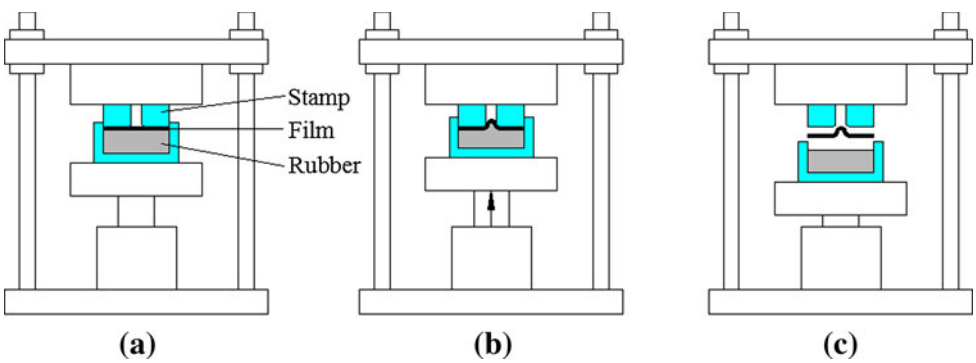

Fig. 1 Rubber-assisted embossing process involving several sequential stages: **a** heating, **b** embossing, holding, and cooling, and **c** mold opening

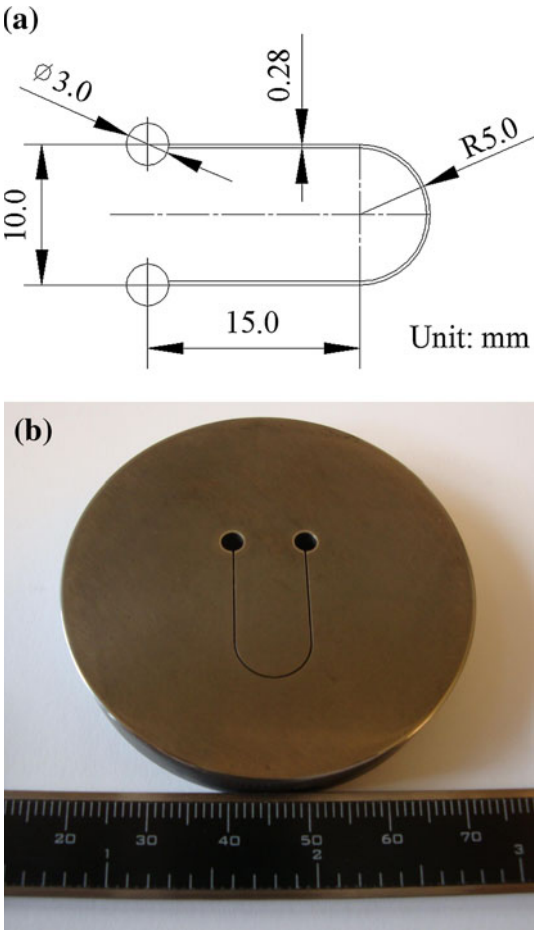

Fig. 2 Embossing stamp with microchannel: **a** microchannel design, **b** actual stamp

3 Results and discussion

In the following sections, the mechanical and rheological behaviors of the embossing film and the rubber pad are presented first, followed by the results from the embossing experiments. The discussion focuses on the correlation of the embossing observations with the rheological properties of the materials involved in this special embossing process.

3.1 Mechanical and rheological properties

Dynamical mechanical analysis was performed to study the deformation behavior of the PS film at different temperatures. The tensile-mode DMA data at a frequency of 1 Hz and a small strain of 1% for the PS film are given in Fig. 3. The temperature during testing was swept from room temperature to about 110°C at which instability occurred. It can be seen that the storage modulus experiences a broad transition around 100°C. If extrapolating the storage modulus along the dot line, one can obtain a vanished value at temperature around 135°C. At this temperature, the polymer is a viscous liquid with a diminished storage modulus.

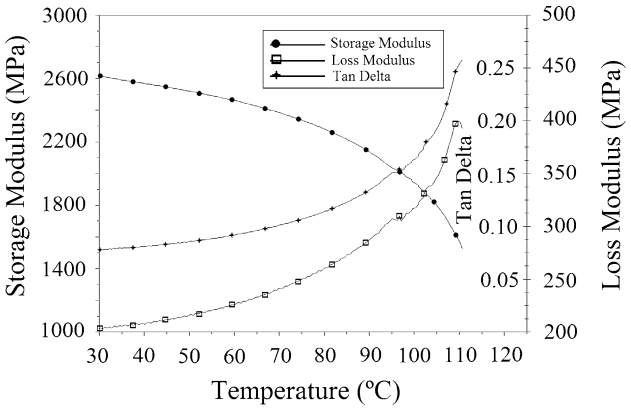

Fig. 3 Temperature-sweep DMA data for PS at 1 Hz

The DMA data for the rubber pads with different Shore hardness varying from 20 to 60 A are shown in Fig. 4. The storage moduli of all these rubber pads are nearly unaffected by the increase in temperature. For each grade of rubber, the loss modulus slightly decreases with the increase in temperature, but its role in affecting the rubber behavior is expected to be little because the storage modulus is more than an order of magnitude higher. These results confirm that the temperature effects on the rubber behavior can be safely neglected.

The hot-chamber tensile test data of PS are shown in Fig. 5. These tests were all conducted isothermally at the testing temperature. For the PS film, a large change in the stress–strain behavior occurs when the temperature increases from 90 to 120°C. At small strain, the Young's moduli were determined to be 439, 158, 9.0, and 1.4 MPa at 90, 100, 110, and 120°C, respectively, indicating strong dependency on temperature. At increased strain, a yielding point is clearly seen at 90°C. The stress–strain curve at 110°C resembles a typical one for an amorphous polymer

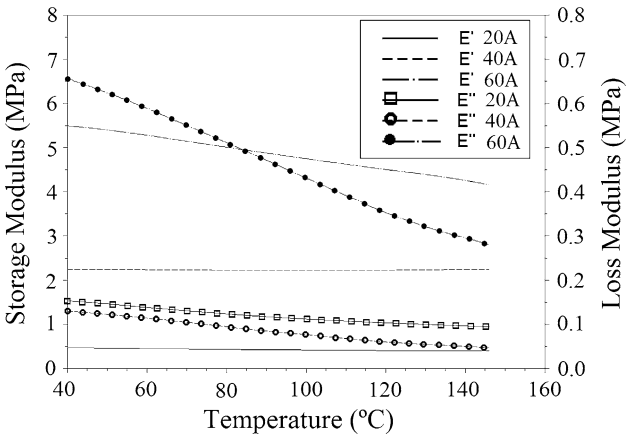

Fig. 4 Temperature-sweep DMA data for silicone rubbers at 1 Hz

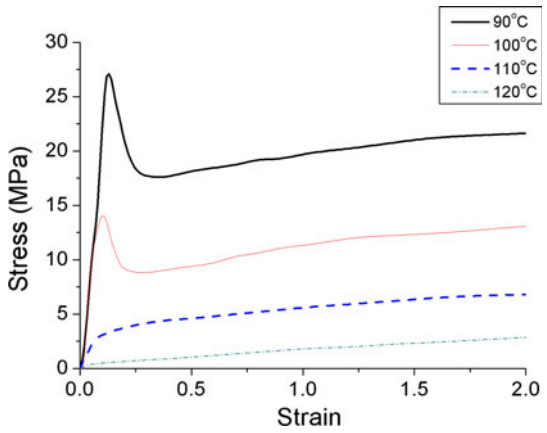

Fig. 5 Tensile stress–strain data of PS at a constant strain rate of 2 s^{-1} and varying testing temperatures

in the rubbery plateau region. The average stress at 110°C is several times lower than that at 90°C. The temperature influence on the tensile testing data agreed with that from the DMA data; both tests showed a transition temperature in the vicinity of 100°C.

3.2 Thickness uniformity

In this study, the main process parameters are embossing temperature, embossing pressure and rubber hardness. The embossing temperature ranges from 90 to 120°C, the embossing pressure ranges from 0.5 to 3.0 MPa, and the hardness of the rubber pads are 20, 40 and 60 A. However, during embossing with the 20 A rubber, it was found that the channel depth was very small when the pressure was less than 1.5 MPa. On the other hand, the rubber was deformed to the point of fracture at the two holes with diameter 3 mm when the pressure was over 1.5 MPa. At the same time, the PS film was also deformed to the breaking point. Therefore, in this case, the 20 A rubber was considered unsuitable for embossing the PS film. In the following experiments, only the 40 A rubber and the 60 A rubber were used in embossing.

Microchannel replication in rubber-assisted embossing using a mold with a through microchannel is illustrated in Fig. 6. It is clearly seen that the mechanical interaction between the PS film and the rubber pad determines the geometry and dimension of the replicated microchannel. Also, the surface roughness of the replicated microchannel is expected to have a significant impact on liquid flow through the microchannel (Zhou and Yao 2011). Figure 7 demonstrates the inner surface of the replicated microchannel. The microchannel was embossed with a 60 A rubber pad at a temperature of 110°C. The embossing pressure was kept at 2.0 MPa. From Fig. 7, it can be seen that the inner surface of microchannel is very smooth. This

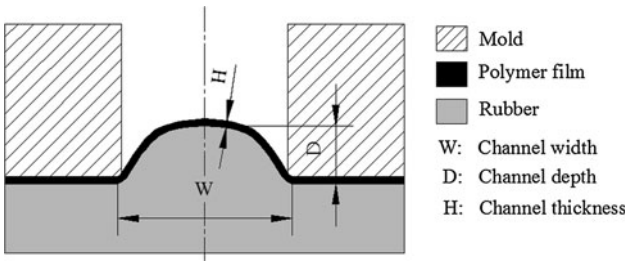

Fig. 6 Microchannel replication in rubber-assisted embossing using a mold with a through microchannel

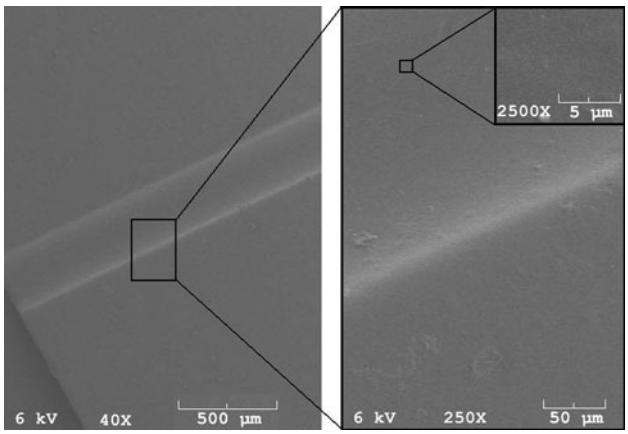

Fig. 7 SEM image of the inner surface of the replicated microchannel

smooth surface finish is understandable because the microchannel surface is deformed against a smooth rubber pad. In contrast, if the microchannel surface is deformed directly by a metal mold, the surface condition of the microchannel mold will play an influential role in affecting the surface finish of the inner microchannel.

The most important process parameter was found to be the embossing temperature. The embossing temperature determines the rheological properties of the embossing film, and more importantly, the relative contrast in mechanical behavior between the polymer film and the rubber pad. Figure 8 compares the uniformity in thickness of the embossed PS films at two different embossing temperatures: 100 and 110°C. The embossing pressure was kept at 2.0 MPa. The rubber pad used in embossing had a Shore hardness of 60 A. It is clearly seen that the channel thickness was much more uniform at the lower embossing temperature. This finding was also explored by measuring the thickness distribution in Fig. 9. The measured data of thickness uniformity was fit by a second-order polynomial. From Fig. 9, it is clearly seen that the replicated thickness became more uniform as the embossing temperature decreased from 120 to 90°C. For deep channel replication, the polymer film should significantly deform in the vertical

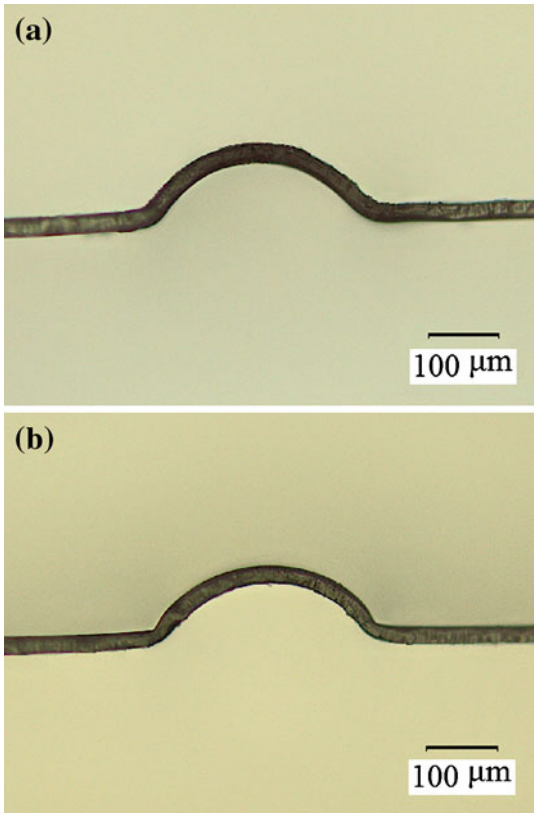

Fig. 8 PS films embossed with a 60 A rubber pad at varied embossing temperatures: **a** 100°C, **b** 110°C. *Scale bar* 100 μm

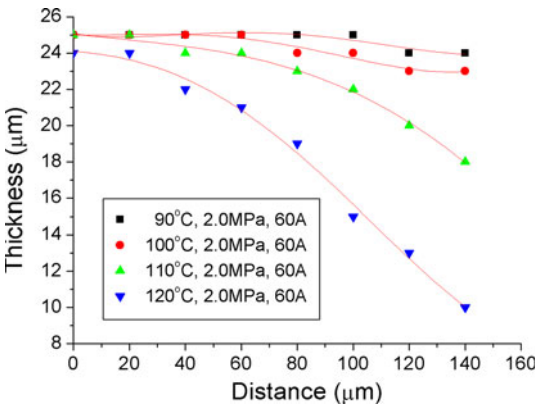

Fig. 9 Thickness distribution of half a channel across the length of the PS film embossed at varied embossing temperatures

direction as the rubber deforms vertically into the channel. There are two possible causes for the thickness non-uniformity. First, from geometrical considerations, the polymer film is expected to experience increased stretching from Point B to Point A (shown in Fig. 5). Second, because the squeeze-type deformation of the rubber pad into the channel could be non-uniform, this would result in non-uniform squeezing of the membrane in the vertical direction and, consequently, a non-uniform thickness distribution.

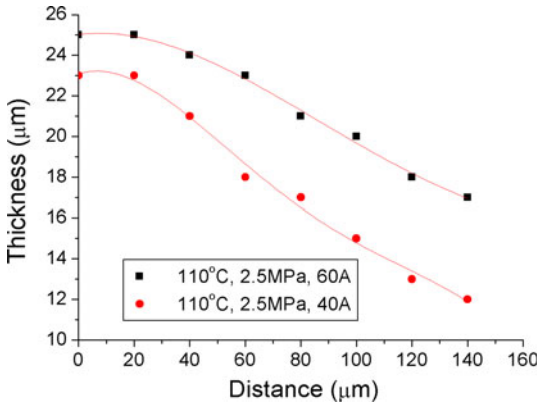

Fig. 10 Thickness distribution of half a channel across the length of the PS film

The results indicated that the second mechanism predominates in the present study. The non-uniform deformation of the rubber would be directly transferred to the polymer film, a softer material, resulting in a non-uniform film thickness. In contrast, the membrane stress at 90°C was almost an order of magnitude higher than that of the rubber stress. Therefore, the rubber pad would behave more like a fluidic medium, and the effect of non-uniform rubber deformation would be minimized at this low embossing temperature.

Rubber pads with different Shore hardness were used in the embossing experiments. Figure 10 compares the thickness distributions for embossing with two different rubber pads of 40 and 60 A hardness. The embossing temperature was 110°C, and the embossing pressure was 2.5 MPa. With the decrease in the Shore hardness, the uniformity in film thickness was reduced. Actually, among all different rubber pads with Shore hardness varying from 20 to 60 A, the best replication quality and film thickness uniformity were obtained at the highest rubber Shore hardness, i.e., 60 A. The reason is that the open-mold configuration in hot embossing can cause squeeze-out of the rubber material in the lateral direction. For the softer rubber pad, it is easier to cause a significant amount of lateral squeezing during embossing. This outward squeeze could reduce the pressure in the microchannel and also change the pressure distribution in the cavity, which ultimately influences the thickness uniformity.

Embossing experiments with varied embossing pressure were also conducted. Figure 11 compares the embossing thickness distributions at embossing pressures of 1.0, 2.0 and 3.0 MPa. The embossing temperature was set to 110°C, and the rubber Shore hardness was 60 A. It can be clearly seen that the uniformity in film thickness was reduced with increasing embossing pressure. The increase in non-uniformity may also be attributed to the increased lateral squeeze flow at increased pressure.

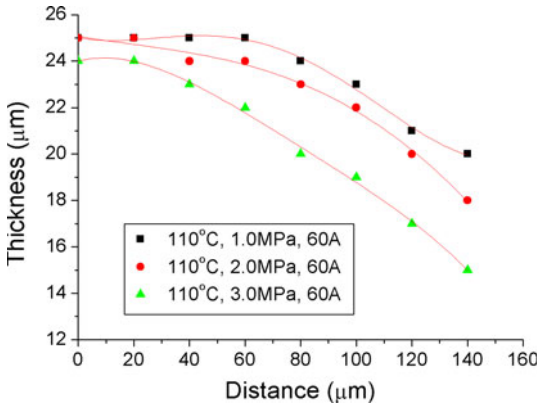

Fig. 11 Effect of embossing pressure on the thickness distribution of half a channel across the length of the PS film

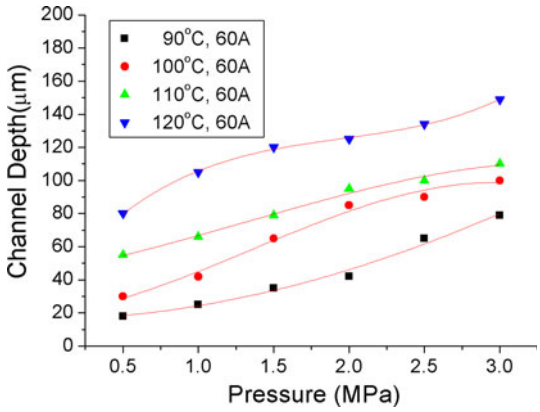

Fig. 13 The relationship of channel depth and embossing pressure at varied embossing temperatures. The rubber Shore hardness is 60 A

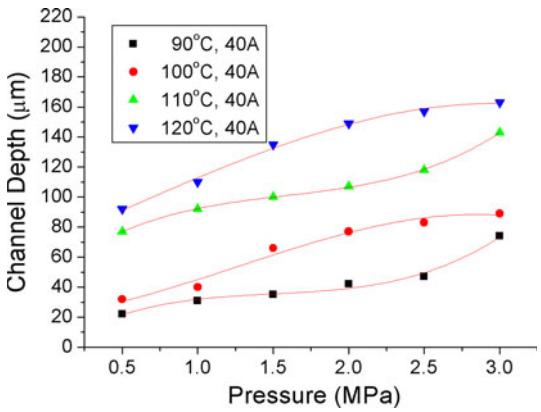

Fig. 12 The relationship of channel depth and embossing pressure at varied embossing temperatures. The rubber Shore hardness is 40 A

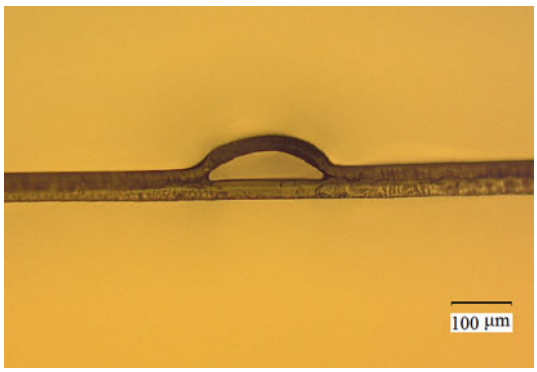

Fig. 14 Cross section of a PS microchannel (channel width 280 μm, channel depth 90 μm, *scale bar* 100 μm)

3.3 Channel depth

Besides the thickness uniformity, the replicated channel depth is also an important quality parameter for the replicated microchannels. Therefore, the channel depth replicated with varied process conditions was also investigated. For the 40 A rubber and the 60 A rubber, the relationships of channel depth and embossing pressure at varied embossing temperatures are shown in Figs. 12 and 13, respectively. A cubic polynomial was used to fit the measured data of channel depth. It is seen clearly that the channel depth is increased with the increase in the embossing pressure at the same embossing temperature. Because more volume of rubber as a soft counter-tool should be pressurized into the microchannel with the increasing pressure, this would result in the increase of channel depth. Furthermore, the channel depth is increased with the increase in the embossing temperature at the same embossing pressure. This can be easily explained considering the reduction of modulus of the polymer film at increased temperatures. During film embossing, it was found that the PS film tended to fracture at point A (shown in Fig. 5) when a high embossing pressure over 5.0 MPa was applied.

3.4 Channel sealing

To test the feasibility of fabricating microfluidic chips using the proposed method, the microchannel thus fabricated was sealed by a transparent adhesive and injected with colored water. Figure 14 shows the cross-section of the microchannel covered with a layer of transparent film. Figure 15 shows the microchannel filled with colored water. The two reservoirs at the start and the end of the U-shaped channel were opened by punching holes through the entire transparent film. A colored water droplet was dispensed in one of the opened reservoirs. As shown in Fig. 15a, the droplet was fast and steadily drawn into the channel by capillary forces and filled the entire channel up to the other opened reservoir. No leakage into the interface between the two films was observed. At the same time, as is shown in Fig. 15b, the microfluidic chip is so flexible that it can be easily bended. These results demonstrated that it is possible to fabricate a longitudinal 3-D microchannel for microfluidic applications

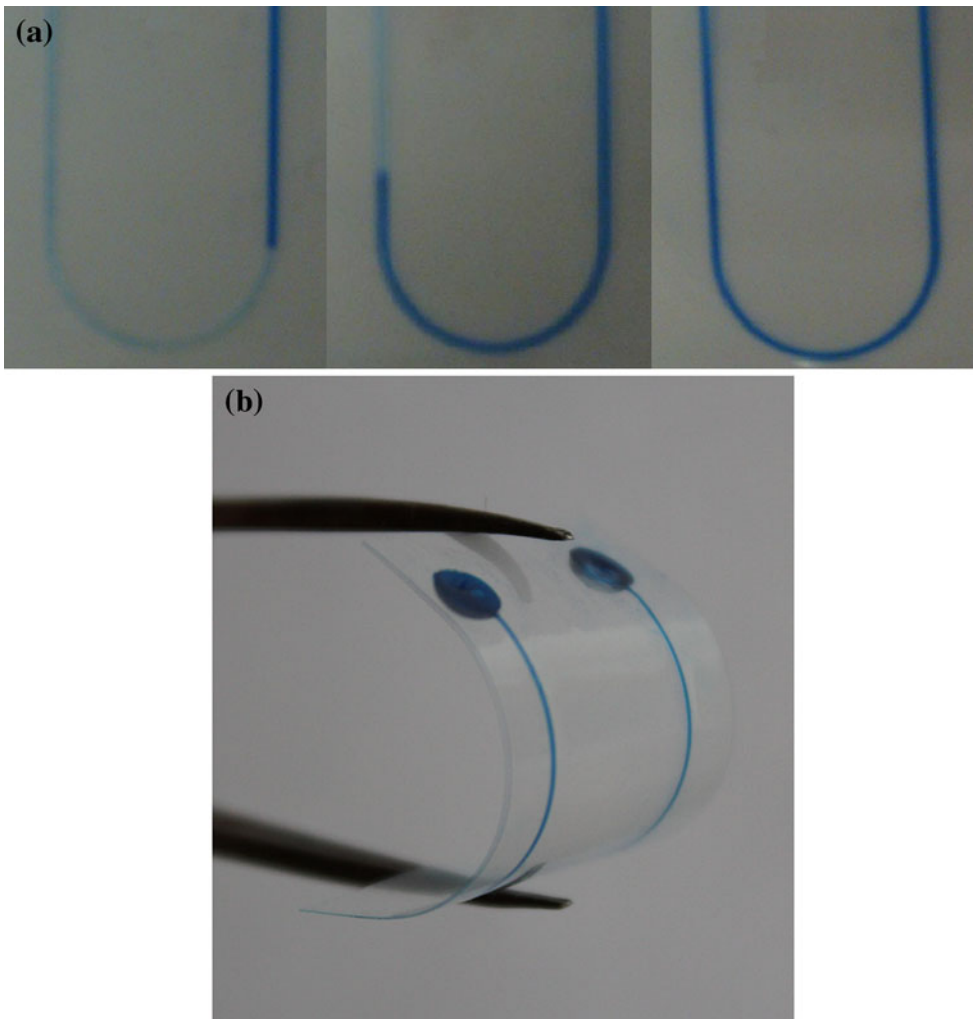

Fig. 15 Microchannel filled with colored water: **a** flow of colored water in microchannel, **b** flexibility of the microchannel

by the rubber-assisted embossing process using a through-thickness microchannel mold.

4 Conclusions

In this study, a rubber-assisted embossing process with a mold containing a through-thickness microchannel was investigated. A thin polymer film is pressurized into the microchannel by the rubber as soft counter-tool. The cavities of the stamp are open to the atmosphere, so it is beneficial to hot embossing of deep microchannels and avoiding the air trap issue. This modification not only simplifies the mold design and fabrication, but also creates smoother surfaces on the embossed articles. The quality of the replicated film in terms of thickness uniformity and channel depth was found to be significantly affected by the embossing temperature, the embossing pressure, and the hardness of the rubber counter-tool. It was observed that the difference in stiffness/hardness between the rubber and the embossing film played an influential role in thickness uniformity and channel depth. An arc-shaped microchannel with a width of 280 μm and the depth of 90 μm was successfully thermoformed using a 25-μm thick PS film at an embossing temperature of 100°C, an embossing pressure of 2.0 MPa, and a rubber Shore hardness of 60 A. Scanning electron microscopy showed that the inner surface of microchannel was very smooth, resulting from deformation against the smooth rubber pad. The experimental results indicated that the channel thickness was much more uniform at the lower embossing temperature. The uniformity in film thickness was reduced with the decrease in the Shore hardness. It was also reduced with the increase in the embossing pressure. On the other hand, the channel depth was increased with the increase in the embossing temperature and the embossing pressure. A flexible microfluidic chip was fabricated via sealing the microchannel with a layer of transparent adhesive film. It was observed that the droplet of colored water was flowing into the microchannel fast and steadily without leaking into the interface. These results demonstrated that the proposed method has the ability of fabricating a flexible 3-D microchannel for special microfluidic chips.

References

Dreuth H, Heiden C (1999) Thermoplastic structuring of thin polymer films. Sens Actuators 78:198–204. doi:10.1016/S0924-4247(99)00237-X

Gates BD, Xu Q, Stewart M, Ryan D, Willson CG, Whitesides GM (2005) New approaches to nanofabrication: molding, printing and other techniques. Chem Rev 105:1171–1196. doi:10.1021/cr030076o

Nagarajan P, Yao DG (2009) Rubber-assisted micro forming of polymer thin films. Microsyst Technol 15:251–257. doi:10.1007/s00542-008-0680-6

Nagarajan P, Yao DG (2011a) Uniform shell patterning using rubber-assisted hot embossing process.I. experimental. Polym Eng Sci 51:592–600. doi:10.1002/pen.21855

Nagarajan P, Yao DG (2011b) Uniform shell patterning using rubber-assisted hot embossing process.I. experimental. Polym Eng Sci 51:601–608. doi:10.1002/pen.21854

Narasimhan J, Papautsky I (2004) Polymer embossing tools for rapid prototyping of plastic microfluidic devices. J Micromech Microeng 14:96–103. doi:10.1088/0960-1317/14/1/013

Rowland HD, Sun AC, Schunk PR, King WP (2005) Impact of polymer film thickness and cavity size on polymer flow during embossing: toward process design rules for nanoimprint lithography. J Micromech Microeng 15:2414–2425. doi:10.1088/0960-1317/15/12/025

Schift H, David C, Gabriel M, Gobrecht J, Heyderman LJ, Kaiser W, Koppel S, Scandella L (2000) Nanoreplication in polymers using hot embossing and injection molding. Microelectron Eng 53:171–174. doi:10.1016/S0167-9317(00)00289-6

Taylor H, Lam YC, Boning D (2010) An investigation of the detrimental impact of trapped air in thermoplastic micro-embossing. J Micromech Microeng 20:0650141. doi:0.1088/0960-1317/20/6/065014

Truckenmuller R, Rummler Z, Schaller T, Schomburg WK (2002) Low-cost thermoforming of micro fluidic analysis chips. J Micromech Microeng 12:375–379. doi:10.1088/0960-1317/12/4/304

Zhou GB, Yao SC (2011) Effect of surface roughness on laminar liquid flow in micro-channels. Appl Therm Eng 31:228–234. doi:10.1016/j.applthermaleng.2010.09.002